Icarus 247 (2015) 95–102

Contents lists available at ScienceDirect

Icarus

journal homepage: www.elsevier.com/locate/icarus

# CXO X-ray spectroscopy of comets and abundances of heavy ions in the solar wind

Vladimir A. Krasnopolsky *

*Department of Physics, Catholic University of America, Washington, DC 20064, USA*
*Moscow Institute of Physics and Technology, Dolgoprudny, Russia*

ARTICLE INFO

*Article history:*
Received 30 June 2014
Revised 18 August 2014
Accepted 12 September 2014
Available online 6 October 2014

*Keywords:*
Comets
Solar wind
Comets, plasma
Spectroscopy

ABSTRACT

X-rays from comets originate in charge exchange between heavy ions of the solar wind and cometary species. Spectra of nine comets observed by the Chandra X-ray Observatory (CXO) are analyzed using the time-dependent instrument sensitivity and the energy-dependent spectral resolution. X-ray emissions are extracted from the spectra in the range of 150–1100 eV using the $\chi^2$-fitting. Production of X-rays varies in the observed comets by a factor of 500 from $4.4 \times 10^{13}$ erg s$^{-1}$ in Comet 73P to $2.2 \times 10^{16}$ erg s$^{-1}$ in Comet Ikeya–Zhang. The measured solar wind flow varies within a factor of 20, being the weakest in Comet 73P and the strongest in 9P/Tempel 1. The retrieved X-ray line intensities vary within a factor of $5 \times 10^4$. These lines above 300 eV are attributed to emissions of the H- and He-like ions, and laboratory data on the excitation cross sections for these emissions (Greenwood et al. [2000]. Astrophys. J. 533, L175–L178) are used to convert the observed emissions into abundances of heavy ions in the solar wind. Continuity equations for charge exchange in comets are solved analytically and result in relationships between the X-ray emissions and the ion fluxes. The flux of $O^{7+}$ scaled to 1 AU varies within a factor of 35 with a mean value of $1.6 \times 10^4$ cm$^{-2}$ s$^{-1}$. The retrieved ratios of $O^{8+}/O^{7+}$, $C^{6+}/C^{5+}$, $Ne^{10+}/Ne^{9+}$, $C^{6+}/O^{7+}$, $N^{6+}/O^{7+}$, and $Ne^{9+}/O^{7+}$ demonstrate significant variations, while their mean values for O, C, and N agree with those recommended by Schwadron and Cravens (Schwadron and Cravens [2000]. Astrophys. J. 544, 558–566) for the slow and fast solar wind. (Data on $Ne^{9+}$ and $Ne^{10+}$ are lacking in Scwadron and Cravens (Schwadron and Cravens [2000]. Astrophys. J. 544, 558–566).) The results are compared with the ion ratios from Bodewits et al. (Bodewits et al. [2007]. Astron. Astrophys. 469, 1183–1195) that were obtained from the same CXO spectra of comets, and some significant differences are briefly discussed. CXO X-ray spectroscopy of comets is a diagnostic tool to study the composition of the solar wind and its variations.



## 1. Introduction

X-ray and EUV emissions from comets were discovered (Lisse et al., 1996; Krasnopolsky et al., 1997) using the Roentgen Satellite (ROSAT) and Extreme Ultraviolet Explorer (EUVE) orbiting observatories. The phenomenon was puzzling, because a ratio of the observed high energy emission to the visible light from comets appeared exceeding that for the Moon by a few orders of magnitude. The first observations were spectrally unresolved (Mumma et al., 1997; Krasnopolsky et al., 2000) or had a very low resolving power $E/\delta E \approx 1$–2 (Dennerl et al., 1997; Owens et al., 1998; $E$ is the photon energy) and could study morphology of the phenomenon and give simple two-parameter spectra of the observed comets. Thermal bremsstrahlung was the most convenient two-parameter presentation (Dennerl et al., 1997; Krasnopolsky, 1998), although thermal bremsstrahlung with a typical temperature of $\sim$300 eV $\approx 3 \times 10^6$ K cannot exist in the very cold comas with $T \approx 70$ K.

Fourteen processes of the X-ray excitation in the cometary gas and dust were considered by Krasnopolsky (1997), and only two of them, scattering by the attogram dust particles and charge transfer of heavy ions in the solar wind, could provide emissions comparable with those measured. Excitation of the X-ray and EUV emissions from comets by charge transfer between heavy ions of the solar wind and neutral molecules and atoms in comets was proposed by Cravens (1997, 2002). These emissions were detected for the first time in the EUVE spectra of Comet Hyakutake with resolving power $E/\delta E \approx 10$ (Krasnopolsky and Mumma, 2001).

* Address: Department of Physics, Catholic University of America, Washington, DC 20064, USA.

http://dx.doi.org/10.1016/j.icarus.2014.09.026
0019-1035/

The solar wind originates in the solar corona with a temperature of a few million degrees. Heavy ions of C, N, O, Ne, etc. constitute $\sim 10^{-3}$ of the solar wind composition. These species are completely or almost completely ionized at these temperatures. Strong electric field of, say, the oxygen nucleus $O^{8+}$ captures an electron from a nearby cometary molecule (mostly $H_2O$):

$$O^{8+} + H_2O \rightarrow O^{7+} + H^+ + OH + 853 \text{ eV}.$$

The released energy results in excitation of $O^{7+}$ that emits an X-ray photon. This is a so-called single electron capture that dominates in the X-ray excitation in comets and, according to the detailed reviews by Krasnopolsky et al. (2004) and Dennerl (2010), is responsible for more than 90% of the X-ray emission. Scattering of the solar X-ray by attogram dust, electron impact and bremsstrahlung, collisions between interplanetary and cometary dust and other excitation processes may contribute a few percent or less.

Recent progress on the problem is related to the observations using the Chandra X-ray Observatory (CXO) in USA and the X-ray Multi-Mirror Newton Observatory (XMM) in Europe. The Advanced CCD Imaging Spectrometer (ACIS) at CXO has an effective area of $\sim 300$ cm$^2$ (Fig. 1) and resolving power of $E/\delta E = 7.5$ near 500 eV. Some tools developed by Krasnopolsky et al. (2002) for analysis of the CXO/ACIS observations of Comet McNaught-Hartley (C/1999 T1) made it possible to extract the comet emissions that were similar to those in a synthetic spectrum by Kharchenko and Dalgarno (2001). This resulted in the first quantitative X-ray spectroscopy of a comet by Kharchenko et al. (2003). That technique was extended to more species and applied to four CXO observations of comets by Krasnopolsky (2006, hereafter Kr06).

An alternative approach to the analysis of the CXO observations of comets was developed by Bodewits et al. (2007, hereafter B07), who studied the data for eight comets. Later Christian et al. (2010) and Lisse et al. (2013) applied the technique of Bodewits et al. (2007) to three other comets. Relative abundances of heavy ions in the solar wind that impacted the comets during the observations are the main products in both Kr06 and B07.

Laboratory data and theoretical calculations of X-ray emission cross sections in charge transfer do not cover all combinations of species and all collision energies. Evidently these data have some uncertainties and sometimes significant differences. (A review of the problem may be found in Krasnopolsky et al. (2004).)

Naturally the results of Kr06 and B07 are different as well and reflect uncertainties in the interpretation of the same observational data. Here we will make some adjustments to our method, extend it to almost all comets observed by CXO, and compare with the results of B07, Christian et al. (2010), and Lisse et al. (2013). The retrieved ion abundance ratios in the solar wind impacting the comets are compared with those derived by Schwadron and Cravens (2000) for the slow and fast solar wind using data from mass spectrometers and some theoretical considerations. The observed composition of the solar wind and its variations will be briefly discussed.

The XMM observations (Dennerl et al., 2003, 2006) resulted in the best X-ray spectrum of comet with resolving power of $\sim 10$ (Comet LINEAR (C/2000 WM1)) and a unique spectrum of Mars with resolved X-ray emissions.

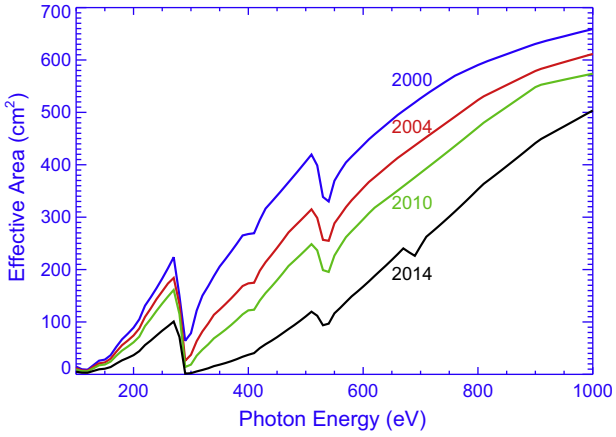


**Fig. 1.** Evolution of the ACIS-S3 effective area because of a hydrocarbon condensation on the optical blocking filter. From the CXO Proposer's Observatory Guide (2014).

## 2. Observations

ACIS has ten CCD chips, and the CXO observations of comets were conducted using a back-illuminated CCD chip S3 as the most sensitive to the soft X-rays. The instrument makes X-ray images of a sky region of interest with a spatial resolution of 0.5 arcsec. Though X-ray emissions from comet appear much stronger than expected initially, comets are actually very faint sources of X-rays. Therefore this spatial resolution cannot be achieved for comets because of poor photon statistics. Signals from the absorbed photons are proportional to their energies, and this makes it possible to retrieve spectra with $E > 150$ eV and resolving power $E/\delta E \approx 7$ near 500 eV. X-ray images of all observed comets were made by averaging of the observed data and published in the original papers. These images of comets with high gas production show bean-like shapes shifted from the nuclei to the Sun. Comas in X-rays for low gas production are more symmetric with minor shifts. Here we will study the observed spectra and will not discuss the X-ray images.

A summary of the observing conditions for each comet is given in Table 1. It includes observing dates, heliocentric and geocentric distances, and phase angles. Heliographic latitudes may be essential as well, because the solar wind is typically slow at the low latitudes and fast at the high latitudes. Gas production rates during the CXO observations are taken from the original CXO publications cited in the table footnotes. Effective aperture reflects the S3 chip size of 8.3 arcmin and is given in km. Exposure times, total count numbers, and count rates are given as well.

Comet LINEAR (C/1999 S4) was observed on July 14 and August 1 2000 before and after a breakup of the nucleus. The gas production and X-ray emission became weak after the breakup, and, similar to Kr06 and B07, we will only consider the data on July 14.

Comet McNaught-Hartley (C/1999 T1) was observed in five one-hour exposures between January 8 and 15, 2001. Similar to the previous works, all data are summed up.

Comet Ikeya–Zhang (153P/2002) was very bright and observed with a fixed pointing while different parts of the comet were passing through the instrument field of view. We chose a period of 7 ks when the brightest part of the coma was observed. This differs from B07 who analyzed the full sum of the observing data.

Comet Tempel 1 (9P/2005) was observed on seven dates before, during, and after the Deep Impact event with a huge total exposure of $\sim 300$ ks. Similar to B07, we chose the observations on June 30 2005, when the comet was the brightest in X-rays.

Comet Tuttle (8P/2008) was observed on January 1, 3, and 4 2008, and the comet was much brighter on January 1 than that on the other dates (Christian et al., 2010). This was caused by strong decrease in the solar wind between the dates. Therefore we will analyze only the data on January 1.

Comet Hartley 2 (103P/2010) was observed on October 17 and November 4, 5, and 16 2010. Again, the comet was much brighter in X-rays on November 4 and 5 (Lisse et al., 2013), and the observing data on these dates are chosen for our analysis.

**Table 1**
Observing conditions.

| Parameter | 1999 S4 LINEAR | 1999 T1 MH | 153P/2002 Ikeya–Zhang | 2P/2003 Encke | 2001 Q4 NEAT | 9P/2005 Tempel 1 | 73P/2006 SW3-B | 8P/2008 Tuttle | 103P/2010 Hartley 2 |
|---|---|---|---|---|---|---|---|---|---|
| Date | 2000/7/14 | 2001/1/8–15 | 2002/4/15–16 | 2003/12/24 | 2004/5/12 | 2005/6/30 | 2006/5/23 | 2008/1/1 | 2010/11/4–5 |
| Heliocentric distance, AU | 0.80 | 1.26 | 0.82 | 0.88 | 0.96 | 1.51 | 0.97 | 1.10 | 1.06 |
| Geocentric distance, AU | 0.53 | 1.37 | 0.45 | 0.28 | 0.38 | 0.88 | 0.10 | 0.25 | 0.16 |
| Phase angle[a] | 98° | 43° | 101° | 104° | 86° | 41° | 114° | 57° | 59° |
| Heliographic latitude | 29.7° | 7.1° | 26° | 11.4° | −3.4° | 0.8° | 0.5° | 3° | −2.5 |
| Gas production rate, $s^{-1}$ [b] | $4 \times 10^{28}$ | $10^{29}$ | $2 \times 10^{29}$ | $7 \times 10^{27}$ | $2 \times 10^{29}$ | $9 \times 10^{27}$ | $2 \times 10^{28}$ | $2 \times 10^{28}$ | $10^{28}$ |
| Exposure, ks | 9.4 | 16.9 | 7.0[c] | 54 | 10.5 | 53 | 20 | 25.9[c] | 37.7[c] |
| Total counts[d] | 11,627 | 16,276 | 82,769 | 10,464 | 9068 | 11,774 | 7548 | 9788 | 16,085 |
| Count rate, cts $s^{-1}$ | 1.238 | 0.964 | 11.77 | 0.194 | 0.863 | 0.220 | 0.362 | 0.377 | 0.426 |
| Effective aperture radius, $\times 10^4$ km | 10.8 | 28 | 9.2 | 5.7 | 7.7 | 18 | 2.1 | 5.2 | 3.3 |

[a] Sun–comet–Earth angle.
[b] Gas productions rates are from Krasnopolsky (2006) for Comets S4, MH, Encke, and Q4; from Bodewits et al. (2007) for Comets 153P, 9P, and 73P; from Christian et al. (2010) for 8P; from Lisse et al. (2013) for 103P.
[c] Some part of the total exposure is analyzed.
[d] At 150–1100 eV and corrected for the background.

Comet LINEAR (C/2000 WM1) was observed using a combination of ACIS and the Low-Energy Transmission Grating (LETG). This combination provides resolving power of $E/\delta E \approx 500$ near 500 eV for point sources. However, comets are extended sources with a typical size of a few arcmin. This results in a degradation of the resolving power to a value, which is close to the ambient ACIS-S3 resolution. An effective area of the ACIS–LETG combination is very much smaller than that of ACIS-S3, and the only useful observing data were those in the zeroth diffraction order that were analyzed by B07 using the ambient ACIS-S3 resolution. However, efficiency of LETG as a function of photon energy in the zeroth diffraction order is unknown, and we will not analyze that observation.

Comet Holmes (17P/2007) was observed using CXO on October 31 2007 with exposure time of 30 ks. The observed signal was very weak, and even the detection is questionable (Christian et al., 2010). We will not analyze that observation.

Comets Encke (2P/2003), NEAT (C/2001 Q4), and Schwassmann–Wachmann 3B (73P/2006) will be analyzed using the full CXO exposures (Table 1).

It is mentioned above that the observations of Comets Tempel 1, Tuttle, and Hartley 2 are analyzed only for dates when the solar wind was comparatively strong. These comets had low gas production during the CXO observations, and their X-ray spectra are very noisy for the weak solar wind. This may make some perturbation in the solar wind statistics. The similar approach was applied by B07.

## 3. Analysis

Here we will briefly discuss our analysis of the CXO spectra of comets and compare it with some features of that in B07. First of all, we need the ACIS-S3 instrument properties: effective area, spectral resolution, and background, all as functions of photon energy.

Evolution of the S3 effective area is shown in Fig. 1. It is caused by a hydrocarbon condensation on the optical blocking filter that rejects the visible and UV photons and is cooled to 120 K. This degradation of the instrument sensitivity is interpolated to the observing dates of all comets.

The current Proposers' Observatory Guide gives the S3 chip spectral resolution of 95 and 150 eV as full widths at half maxima (FWHM) at 1.49 and 5.9 keV, respectively. Fitting of these values by a power function gives

$$\mathrm{FWHM} = 83E^{1/3}\ \mathrm{eV}.$$

Here the photon energy $E$ is in keV, and the spectral resolution varies from 56 to 83 eV at the photon energies of 300 and 1000 eV, respectively. We apply this variable spectral resolution to our synthetic spectra. (B07 just mentioned that the instrument spectral resolution is ~50 eV in the 300–1500 eV energy range.)

Data on the instrument background are very essential for a range of 700–1100 eV, where the signal from comets is weak and comparable to the background. This problem is especially critical for faint comets, that is, five of nine comets in Table 1. Kr06 subtracted a signal near the edges of the S3 chip from that in the central part. This worsened the photon statistics but could provide a careful correction for the background that was accepted uniform on the chip, while the cometary photons were mostly near the chip center. However, this method is not applicable to the faint comets. B07 took the background from another back-illuminated chip S1 that was switched on simultaneously with S3. Our test of this possibility is not encouraging. Evidently the S1 and S3 properties are rather different, and their backgrounds are different as well.

Christian et al. (2010) considered a few versions of the background, and their results were sensitive to the chosen versions. Here we will apply a spectrum of the background from the Proposers' Observatory Guide (2014) that includes the diffuse X-ray component after exclusion of all point sources (Fig. 2). Comparing this background with spectra of comets at 1100–1400 eV, where the expected cometary emissions are negligible, we see

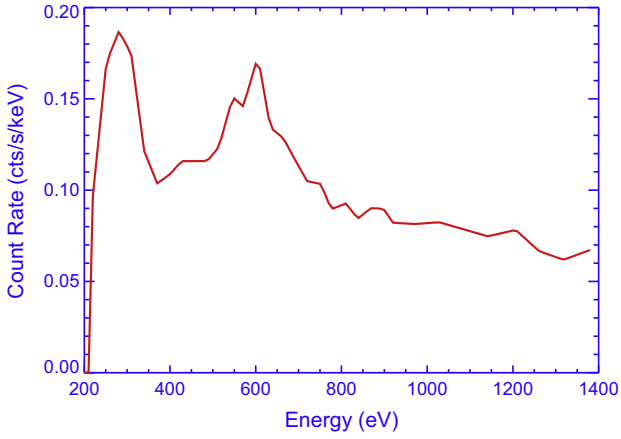


**Fig. 2.** The S3 background spectrum.

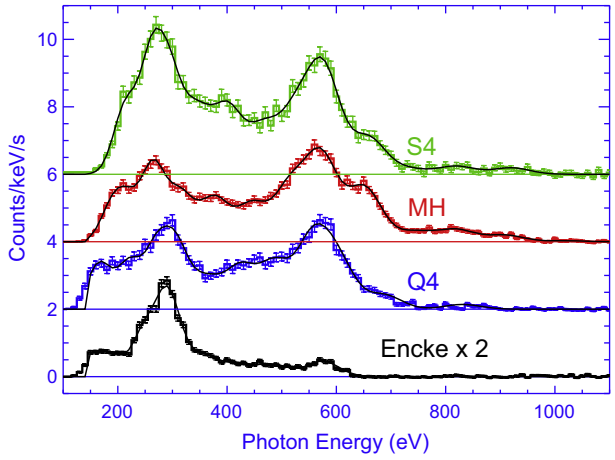


**Fig. 3.** Background-corrected spectra of four comets. Best fit models to the spectra are shown by thin black lines. The zero levels are shifted and shown by the straight lines.

some excess over the background. This excess may be due to weak X-ray sources in the field of view. Therefore we subtract the background spectrum (Fig. 2) that is scaled to a spectrum of comet at 1100–1400 eV.

The background-corrected spectra of four comets from the CXO list are shown in Fig. 3 with energy intervals of 10 eV. They are not identical to the similar spectra in Kr06 (Fig. 1). For example, the peak at 280 eV is greater in Comet S4 than that at 570 eV in the current version while being smaller in Kr06. Overall, the background subtraction in Kr06 might be better but cannot be applied to five faint comets from our list. We prefer to process the spectra of all comets similarly, and the chosen background subtraction looks the best though not perfect.

The background-corrected spectra are $\chi^2$-fitted by sets of narrow emission lines with their photon energies and intensities as free parameters. The S3 effective area as a function of time (Fig. 1) is interpolated to time of the observation. The adopted emission line spectrum is scaled by the S3 effective area and then convolved with a few Gaussians with FWHM between 50 and 100 eV. The final spectrum is interpolated in accord with the variable instrument spectral resolution, and the result is compared to the observed spectrum. Then the parameters are adjusted to minimize the difference. The final difference corrected to the number of degrees of freedom (the number of the energy intervals minus twice the number of the lines) gives $\chi^2 \approx 1$–1.5, that is, the model is statistically plausible. The calculated model spectra (Fig. 3) are almost undistinguishable from the observed spectra. Our analysis of the spectra is extended to 150 eV, while the standard CXO tools and the results of B07 begin at 300 eV.

Results of this fitting for all nine comets are shown in Table 2. Uncertainties of the photon energies $E$ and emission intensities $I$ are calculated assuming that one-sigma deviations of $E$ and $I$ result in increases in $\chi^2$ by factors $1 + 1.8/n$ and $1 + 0.4/n$, respectively (Kr06). Here $n$ is the number of lines in a spectrum.

## 4. Ion abundance ratios

In this section we will retrieve ion abundance ratios in the solar wind near the observed comets using the X-ray emissions from Table 2 and emission cross sections for the single electron capture from the laboratory studies.

The best-fit model spectra of four comets are compared in Fig. 4 with a synthetic spectrum of the solar wind charge exchange in a comet that was calculated by Kharchenko and Dalgarno for

**Table 2**
X-ray emissions from comets.

| S4 LINEAR | | T1 MH | | 153P/Ikeya-Z | | 2P/Encke | | Q4 NEAT | | 9P/Tempel1 | | 73P/SW3-B | | 8P/Tuttle | | 103P/Hartley 2 | |
|---|---|---|---|---|---|---|---|---|---|---|---|---|---|---|---|---|---|
| $E$ (eV) | $I$ | $E$ (eV) | $I$ | $E$ (eV) | $I$ | $E$ (eV) | $I$ | $E$ (eV) | $I$ | $E$ (eV) | $I$ | $E$ (eV) | $I$ | $E$ (eV) | $I$ | $E$ (eV) | $I$ |
| 214 ± 3 | 75 ± 4 | 190 ± 3 | 384 ± 20 | 151 ± 3 | 763 ± 46 | 147 ± 5 | 16 ± 1.6 | 165 ± 3 | 80 ± 6 | 221 ± 5 | 33 ± 3 | 200 ± 4 | 0.8 ± 0.1 | 189 ± 3 | 20 ± 1 | 194 ± 2 | 8 ± 0.4 |
| 264 ± 3 | 72 ± 4 | 219 ± 4 | 234 ± 15 | 196 ± 3 | 258 ± 13 | 190 ± 5 | 5.2 ± 0.4 | 221 ± 5 | 26 ± 2 | 276 ± 2 | 142 ± 7 | 215 ± 3 | 1.7 ± 0.1 | 255 ± 3 | 9 ± 0.5 | 261 ± 2 | 5 ± 0.2 |
| 300 ± 3 | 140 ± 10 | 266 ± 2 | 326 ± 12 | 243 ± 3 | 143 ± 7 | 248 ± 4 | 5.0 ± 0.3 | 273 ± 9 | 23 ± 2 | 312 ± 3 | 111 ± 1 | 267 ± 2 | 1.9 ± 0.1 | 290 ± 2 | 70 ± 5 | 306 ± 2 | 16 ± 1 |
| 350 ± 5 | 40 ± 3 | 318 ± 3 | 333 ± 16 | 296 ± 2 | 970 ± 28 | 293 ± 3 | 48 ± 2 | 309 ± 3 | 64 ± 5 | 358 ± 7 | 27 ± 3 | 311 ± 3 | 2.9 ± 0.2 | 336 ± 5 | 8 ± 1 | 373 ± 6 | 2 ± 0.8 |
| 404 ± 5 | 37 ± 3 | 379 ± 3 | 195 ± 9 | 355 ± 3 | 152 ± 7 | 362 ± 6 | 2.8 ± 0.2 | 368 ± 8 | 15 ± 2 | 427 ± 9 | 12 ± 2 | 374 ± 4 | 0.8 ± 0.05 | 387 ± 7 | 3 ± 0.3 | 439 ± 7 | 1 ± 0.05 |
| 468 ± 7 | 20 ± 2 | 447 ± 9 | 130 ± 6 | 413 ± 3 | 162 ± 6 | 424 ± 8 | 1.2 ± 0.3 | 426 ± 6 | 16 ± 1.3 | 494 ± 10 | 8 ± 1 | 442 ± 6 | 0.37 ± 0.03 | 451 ± 7 | 2.1 ± 0.2 | 505 ± 6 | 1 ± 0.04 |
| 527 ± 5 | 28 ± 2 | 517 ± 3 | 164 ± 7 | 476 ± 3 | 149 ± 5 | 487 ± 8 | 0.9 ± 0.1 | 488 ± 6 | 13 ± 1.0 | 568 ± 6 | 15 ± 1 | 503 ± 9 | 0.18 ± 0.03 | 506 ± 10 | 1.5 ± 0.2 | 573 ± 4 | 1.7 ± 0.1 |
| 578 ± 4 | 42 ± 4 | 574 ± 2 | 252 ± 8 | 538 ± 2 | 273 ± 8 | 575 ± 7 | 1.1 ± 0.1 | 558 ± 5 | 20 ± 1.3 | 654 ± 11 | 5 ± 1 | 569 ± 5 | 0.36 ± 0.02 | 569 ± 5 | 3 ± 0.2 | 643 ± 9 | 0.4 ± 0.05 |
| 660 ± 7 | 13 ± 1 | 653 ± 3 | 138 ± 5 | 595 ± 2 | 356 ± 13 | | | 605 ± 6 | 10 ± 1 | 775 ± 21 | 2.3 ± 0.5 | 631 ± 30 | 0.04 ± 0.01 | 638 ± 28 | 0.6 ± 0.1 | 713 ± 14 | 0.2 ± 0.03 |
| 735 ± 38 | 1.7 ± 0.7 | 747 ± 10 | 23 ± 3 | 668 ± 2 | 256 ± 5 | | | 688 ± 10 | 3.0 ± 0.4 | 879 ± 36 | 0.9 ± 0.4 | 682 ± 50 | 0.02 ± 0.01 | 724 ± 26 | 0.3 ± 0.1 | 826 ± 17 | 0.1 ± 0.02 |
| 820 ± 23 | 2.6 ± 0.6 | 820 ± 8 | 27 ± 2 | 750 ± 6 | 46 ± 3 | | | 831 ± 18 | 0.9 ± 0.2 | 967 ± 47 | 0.7 ± 0.4 | | | | | 964 ± 17 | 0.07 ± 0.02 |
| 920 ± 22 | 2.0 ± 0.6 | 909 ± 12 | 14 ± 2 | 813 ± 3 | 72 ± 3 | | | | | | | | | | | | |
| | | 1019 ± 33 | 2.1 ± 1.3 | 887 ± 4 | 48 ± 2 | | | | | | | | | | | | |
| | | | | 958 ± 7 | 15 ± 1 | | | | | | | | | | | | |
| | | | | 1052 ± 6 | 11 ± 1 | | | | | | | | | | | | |
| Total | $4.8 \times 10^{24}$ | $2.2 \times 10^{25}$ ph/s | | $3.7 \times 10^{25}$ ph/s | | $8.1 \times 10^{23}$ ph/s | | $2.7 \times 10^{24}$ ph/s | | $3.6 \times 10^{24}$ ph/s | | $9.0 \times 10^{22}$ ph/s | | $1.2 \times 10^{24}$ ph/s | | $3.6 \times 10^{23}$ ph/s | |
| | $2.7 \times 10^{15}$ | $1.3 \times 10^{16}$ erg/s | | $2.2 \times 10^{16}$ erg/s | | $3.4 \times 10^{14}$ erg/s | | $1.3 \times 10^{15}$ erg/s | | $1.8 \times 10^{15}$ erg/s | | $4.4 \times 10^{13}$ erg/s | | $5.5 \times 10^{14}$ erg/s | | $1.8 \times 10^{14}$ erg/s | |

Line intensities $I$ are in $10^{22}$ ph/s.

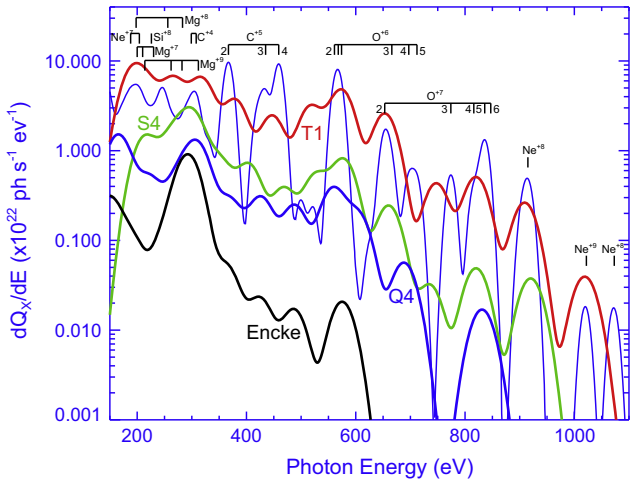


**Fig. 4.** Best-fit model spectra of four comets convolved by a Gaussian with FWHM = 50 eV. Thin line is a synthetic X-ray spectrum of a comet by Kharchenko and Dalgarno for the slow solar wind and convolved by a Gaussian with FWHM = 20 eV. Positions, identifications, and principal quantum numbers of the emission lines are shown.

Krasnopolsky et al. (2002) using the composition of the slow solar wind from Schwadron and Cravens (2000). (Fig. 4 is similar but not identical to Fig. 3 in Kr06) Photon energies of the lines in the spectra are rather close to the expected values in the synthetic spectrum. This makes it possible to identify the lines and perform quantitative spectroscopy.

The solar wind is a highly variable phenomenon, and ion abundance ratios present its composition better than absolute ion abundances. Furthermore, some errors cancel out in the ratios. Abundances of the bare nuclei $Ne^{10+}$, $O^{8+}$, $N^{7+}$, and $C^{6+}$ and one-electron ions $Ne^{9+}$, $O^{7+}$, $N^{6+}$, and $C^{5+}$ may be extracted from the spectra of comets.

The bare nuclei result in hydrogen-like ions after the single electron capture from a cometary species that is mostly $H_2O$. These ions emit Lyman-α, β, and γ + δ + ε; the latter are not separated by the S3 resolution, and we consider three lines from each ion. Emission cross sections of the hydrogen-like ions (Table 3) are taken from Greenwood et al. (2000, 2001) with relative yields from Kharchenko et al. (2003) for $O^{7+}$ and from Beiersdorfer et al. (2003) for $C^{5+}$ after the electron capture from $CO_2$.

Hydrogen-like ions $Ne^{9+}$, $O^{7+}$, $N^{6+}$, and $C^{5+}$ form helium-like ions after the electron capture from a cometary species ($H_2O$). Excitation of one electron to quantum state $n = 2$ results in three states $^3S_1$, $^3P_1$, and $^1P_1$ and three lines that are unresolved by the instrument, e.g., 561, 568, and 574 eV for $O^{6+}$. The first state is metastable, and the first line may be significantly depleted by quenching in the laboratory studies but not in comets. The emissions from higher $n \geqslant 3$ are weak (Table 3). The $C^{4+}$ emission cross sections in Table 3 are taken from Kr06 for $C^{5+} + H_2$ and scaled to a ratio of those for $C^{6+} + H_2O$ and $H_2$ from Greenwood et al. (2000) and Hoekstra et al. (1989), respectively.

The cross sections in Table 3 are based mostly on the laboratory studies by Greenwood et al. (2000, 2001; see also the review by Krasnopolsky et al., 2004) that were made for the ion velocity ~700 km $s^{-1}$. This may be compared with the solar wind velocity, which typically varies from 300 to 1200 km $s^{-1}$, with a significant deceleration behind the comet bow shock. It is difficult to evaluate uncertainties induced by the emission cross sections measured at 700 km $s^{-1}$. However, they may be significantly reduced in the ion ratios.

We solved the steady-state continuity equations for charge exchange in comets and got the following relationships for emissions from the primary ions (subscript 0) and sums of the primary and secondary ions (subscript 1);

$$I_0 = 2\pi\gamma_0\Phi_0 \int_0^R \left(1 - \exp\left(-\frac{\sigma_0 Q}{4\pi v r}\right)\right) r\, dr;$$

$$I_1 = 2\pi\gamma_1\Phi_1 \int_0^R \left(1 - \exp\left(-\frac{\sigma_1 Q}{4\pi v r}\right)\right) r\, dr + 2\pi\gamma_1\gamma_{01}\Phi_0 \times \int_0^R \left[1 - \frac{\sigma_0 \exp(-\sigma_1 Q/4\pi v r) - \sigma_1 \exp(-\sigma_0 Q/4\pi v r)}{\sigma_0 - \sigma_1}\right] r\, dr.$$

Here $\Phi$ is the ion flux, $\gamma$ is the quantum yield, $\gamma_{01}$ is the yield of the single electron capture, $\sigma$ is the total charge exchange cross section, $Q$ is the gas production rate, $v \approx 1$ km $s^{-1}$ is the gas velocity, and $R$ is the aperture radius.

To simplify the geometry, the above relationships are calculated for a phase angle (Sun–comet–observer angle) of zero. However, the X-ray emission from comets is expected to be almost isotropic, and this approximation is reasonable. The charge exchange cross sections are assumed constant, neglecting deceleration of the solar wind and the associated changes in the cross sections.

Using these relationships with $Q$, $R$ from Table 1 and $\sigma$, $\gamma$ from Table 3, all emissions of the H- and He-like ions may be calculated for fixed ion fluxes. Comparing the calculated emissions with those observed, one gets fluxes of the solar wind ions in the comets.

According to Table 3, the emission at 500–600 eV is a sum of $O^{6+}$ 560 eV and $N^{6+}$ 500 and 593 eV. However, ratios of N/O is ≈0.1 in the solar photosphere and the solar wind, and $N^{7+}/O^{7+} \leqslant 0.03$ in the solar wind (von Steiger et al., 2000; Schwadron and Cravens, 2000; Krasnopolsky et al., 2004). Therefore we neglect the contribution from $N^{7+}$ to the spectra of comets. Then the total emission of $O^{7+}$ is equal to $I_{600-880} - 0.12\ I_{500-600}$. The emissions of $N^{5+}$ and $C^{5+}$ at 430 eV are unresolved, and the $N^{5+}$ emission is equal to $I_{430} - 0.2\ I_{367+460}$. Lines of $Mg^{8+}$ contribute to the emission at 300 eV; therefore the $C^{4+}$ emission is $I_{300} - I_{250}$.

Using these considerations, the absolute ion fluxes are retrieved from the observed X-ray emissions in Table 2. These data are given as fluxes of $O^{7+}$ and ion flux ratios in Table 4.

Uncertainties of the cross sections in Table 3 are ~15% based on the data from Greenwood et al. (2000, 2001). The uncertainties in the intensities from Table 2 add to these values and result in

**Table 3**
Excitation cross sections for single electron capture emission of H- and He-like ions in $H_2O$.

| $Ne^{9+}$ | | $O^{7+}$ | | $N^{6+}$ | | $C^{5+}$ | | $Ne^{8+}$ | | $O^{6+}$ | | $N^{5+}$ | | $C^{4+}$ | |
|---|---|---|---|---|---|---|---|---|---|---|---|---|---|---|---|
| *E* | σ | *E* | σ | *E* | σ | *E* | σ | *E* | σ | *E* | σ | *E* | σ | *E* | σ |
| 1022 | 81 | 654 | 45 | 500 | 34 | 367 | 32 | 915 | 73 | 560 | 47 | 425 | 48 | 300 | 28 |
| 1211 | 10 | 774 | 7 | 593 | 26 | 435 | 10 | 1072 | 3 | 666 | 5.5 | 497 | 3 | 355 | 1.3 |
| 1300 | 9 | 840 | 11 | 630 | 21 | 460 | 17 | 1140 | 4 | 697 | 0.3 | 530 | – | 371 | 0.2 |
| σ2 | 15 | σ2 | 15 | σ2 | 15 | σ2 | 8 | σ2 | 12 | σ2 | 8 | σ2 | – | σ2 | – |

$Ne^{9+}$, $N^{6+}$, $Ne^{8+}$: Greenwood et al. (2000); $O^{7+}$, $O^{6+}$: Kharchenko et al. (2003) scaled to Greenwood et al. (2000); $C^{5+}$: Beiersdorfer et al. (2003, $CO_2$) scaled to Greenwood et al. (2000); $N^{5+}$: Suraud et al. (1991, $H_2$); $C^{4+}$: Kr06 ($H_2$), see text. *E* is the line energy in eV, σ is the emission cross section in $10^{-16}$ $cm^2$, σ2 is the two-electron capture cross section.

**Table 4**
Solar wind ion abundance ratios in comets observed using CXO.

| Value | LINEAR S4 | MH T1 | 153P/IZ | 2P/Encke | Q4 NEAT | 9P/Tempel | 73P/SW | 8P/Tuttle | 103P | Mean | SW | FW |
|---|---|---|---|---|---|---|---|---|---|---|---|---|
| $r^{3/2}Q_X/QR$[a] | 45 | 66 | 29 | 70 | 79 | 206 | 10 | 61 | 60 | 70 ± 55 | – | – |
| $O^{7+}$ | 1.56 + 4 | 3.5 + 4 | 4.24 + 4 | 3.0 + 3 | 3.1 + 3 | 2.9 + 4 | 1.2 + 3 | 5.3 + 3 | 8.5 + 3 | 1.6 + 4 | 2.2 + 4 | 3.5 + 3 |
| $O8^+/O^{7+}$ | 0.10 ± 0.04<br>*0.32 ± 0.03* | 0.26 ± 0.07<br>*0.42 ± 0.04* | 0.47 ± 0.11<br>*0.96 ± 0.04* | <0.02<br>*0.19 ± 0.04* | 0.21 ± 0.10<br>*0.17 ± 0.03* | 0.30 ± 0.10<br>*0.19 ± 0.06* | 0.04 ± 0.03<br>*0.10 ± 0.04* | 0.14 ± 0.06<br>*0.23 ± 0.03* | 0.23 ± 0.07<br>– | 0.22 ± 0.13<br>*0.32 ± 0.28* | 0.35 | 0 |
| $C^{6+}/O^{7+}$ | 0.84 ± 0.18<br>*1.4 ± 0.4* | 0.70 ± 0.15<br>*0.95 ± 0.4* | 0.55 ± 0.15<br>*1.21 ± 0.0* | 3.3 ± 0.8<br>*2.9 ± 1.1* | 1.2 ± 0.3<br>*1.2 ± 0.9* | 2.3 ± 0.5<br>*0.0 ± 0.6* | 3.9 ± 0.9<br>*2.3 ± 1.1* | 1.5 ± 0.3<br>*0.71 ± 0.08* | 1.8 ± 0.6<br>– | 1.8 ± 1.2<br>*1.33 ± 0.91* | 1.6 | 2.8 |
| $C^{6+}/C^{5+}$ | 0.57 ± 0.14<br>*0.12 ± 0.05* | 2.1 ± 0.80<br>*0.06 ± 0.03* | 0.33 ± 0.08<br>*0.13 ± 0.00* | 0.05 ± 0.01<br>*0.05 ± 0.02* | 0.6 ± 0.15<br>*0.025 ± 0.02* | 0.16 ± 0.06<br>*0.0 ± 0.03* | 0.9 ± 0.4<br>*0.03 ± 0.018* | 0.05 ± 0.02<br>*0.01 ± 0.001* | 0.17 ± 0.09<br>– | 0.55 ± 0.65<br>*0.053 ± 0.048* | 1.5 | 0.2 |
| $N^{6+}/O^{7+}$ | 0.34 ± 0.09<br>*0.63 ± 0.21* | 0.17 ± 0.05<br>*0.47 ± 0.20* | 0.17 ± 0.04<br>*0.56 ± 0.0* | 0.39 ± 0.27<br>*0.79 ± 0.55* | 0.41 ± 0.10<br>*1.1 ± 0.52* | 0.32 ± 0.16<br>*0.72 ± 0.48* | 0.38 ± 0.12<br>*1.5 ± 0.72* | 0.38 ± 0.25<br>*1.2 ± 0.12* | 0.22 ± 0.16<br>– | 0.31 ± 0.10<br>*0.87 ± 0.36* | 0.29 | 0.37 |
| $N^{7+}/N^{6+}$ | *0.11 ± 0.10* | *0.40 ± 0.21* | *0.45 ± 0.00* | *0.18 ± 0.21* | *0.23 ± 0.14* | *0.00 ± 0.50* | *0.005 ± 0.050* | *0.29 ± 0.04* | – | *0.21 ± 0.17* | 0.1 | 0 |
| $Ne^{9+}/O^{7+}$ | 0.019 ± 0.007 | 0.023 ± 0.006 | 0.047 ± 0.009 | – | – | 0.031 ± 0.014 | – | – | 0.028 ± 0.01 | 0.030 ± 0.011 | – | – |
| $Ne^{10+}/O^{7+}$ | <0.005<br>*0.02 ± 0.01* | 0.003 ± 0.002<br>*0.004 ± 0.005* | 0.015 ± 0.004<br>*0.01 ± 0.0001* | –<br>*0.05 ± 0.02* | –<br>*0.008 ± 0.004* | <0.015<br>*0.002 ± 0.007* | –<br>*0.001 ± 0.01* | –<br>*0.030 ± 0.020* | <0.004<br>– | 0.009 ± 0.006<br>*0.016 ± 0.017* | – | – |
| $Ne^{10\pm}/Ne^{9+}$ | <0.2 | 0.14 ± 0.09 | 0.32 ± 0.10 | – | – | <0.5 | – | – | <0.25 | 0.23 ± 0.11 | – | – |

Our results are shown solid, those from Bodewits et al. (2007) for seven comets and Christian et al. (2010) for 8P/Tuttle are italic. Uncertainties of the mean reflect variations of the value. SW and FW are the slow and fast solar wind, and the data are from Schwadron and Cravens (2000). The third line shows the retrieved fluxes of $O^{7+}$ in the solar wind, scaled to 1 AU and given in $cm^{-2}\,s^{-1}$; 1.56+4 =$1.56*10^4$ $cm^{-2}\,s^{-1}$.

[a] This value is in $10^{-20}$ erg/km; it is proportional to the heavy ion flux in the solar wind in comets, see text.

uncertainties of the ion ratios that are given in Table 4. The uncertainties of the ion ratios in Table 4 do not include systematic errors associated with some inevitable assumptions in this work.

## 5. Results and discussion

Nine comets observed by CXO cover a great variety of the observing conditions and properties of the comets and the solar wind. Gas production rate (Table 1) varies within a factor of 30, being minimal for Comet Encke and maximal for Ikeya–Zhang. X-ray count rate varies for these comets by a factor of 60.

Total X-ray emissions of the comets are retrieved in photons and ergs per second for the range of 150–1100 eV (Table 2). These emissions vary by a factor of 500 from $4.4 \times 10^{13}$ erg $s^{-1}$ for Comet 73P to $2.2 \times 10^{16}$ erg $s^{-1}$ for Ikeya–Zhang. The greatest X-ray emission in the ROSAT survey (Dennerl et al., 1997) was at $1.16 \times 10^{16}$ erg $s^{-1}$ in Comet Levy (C/1990 K1).

Intensities of individual lines vary within a spectrum by a factor of 200. Comparing the weakest and strongest emissions in Table 2, the difference is a factor of $5 \times 10^4$.

X-ray emission $Q_X$ from a comet is proportional to the solar wind flow $\Phi_0/r^2$ and an abundance $M$ of molecules in the coma within an aperture with radius $R$: $M = \pi QR/2V$. Here $\Phi_0$ is the solar wind flow at 1 AU, $r$ is the heliocentric distance, $Q$ is the gas production rate, and $V = V_0 r^{-1/2}$ (Cochran and Schleicher, 1993) is the gas velocity in the coma. This means that the solar wind flux at 1 AU is proportional to $r^{3/2}\,Q_X/QR$, and these values for nine comets are given in Table 4. The solar wind was the strongest in the observations of Comet Tempel 1 and the weakest for Comet 73P; their ratio is a factor of 20.

The above consideration is valid for collisionally thin comas. Using the charge exchange cross section of $10^{-15}$ $cm^2$, radius of the collisionally thick coma of Ikeya–Zhang is 5000 km, much smaller that the aperture of 92,000 km. Comet Ikeya–Zhang is the most active; therefore this approximation is valid for all comets in the CXO list.

The observed fluxes of $O^{7+}$ are scaled to 1 AU in Table 4. (These data are lacking in Kr06 and B07.) They vary by a factor of 35 from 1200 to $4.2 \times 10^4$ $cm^{-2}\,s^{-1}$ in Comets 73P and Ikeya–Zhang, respectively. Ratios of $O^{7+}$ in the total flux of heavy ions $r^{3/2}\,Q_X/QR$ varies also by a factor of 35, being the lowest in Comet Q4.

The mean solar wind flow is $2.5 \times 10^8$ $cm^{-2}\,s^{-1}$ at 1 AU, and heavy ions constitute $\sim 10^{-3}$ of this flow (Cravens, 1997). Then mean fluxes of $O^{7+}$ in the slow and fast winds are equal to those in Table 4 using the data of Schwadron and Cravens (2000). The mean $O^{7+}$ flux from this work is between these values.

The retrieved ion abundance ratios during the CXO observations of comets are compared in Table 4 with those calculated by Schwadron and Cravens (2000) for the slow and fast solar wind. Ratios of the same ions vary significantly from comet to comet, and their mean values and standard deviations are given in Table 4 as well. These mean values are in excellent agreement with those from Schwadron and Cravens (2000). The standard deviations are not uncertainties of the mean values but reflect variabilities of the ion ratios. Comparing the ion ratios in each comet with those in the slow and fast solar wind, we conclude that the wind was slow in Comets McNaught-Hartley and Ikeya–Zhang, fast in Comets Tempel 1 and 73P/SW, and intermediate in the other five comets. Our set of the data is insufficient to indicate a direct correlation of the solar wind velocity with heliographic latitude.

Data on $Ne^{9+}$ and $Ne^{10+}$ in the solar wind are lacking in Schwadron and Cravens (2000). Our analysis gives the mean $Ne^{9+}/O^{7+} = 0.03$ and $Ne^{10+}/Ne^{9+} = 0.23$.

Using the measured degrees of ionization of the same species, it is possible to get temperatures of the solar wind ion formation in the solar corona. This may be made assuming thermodynamic equilibrium and either solving the Saha equation or using numerical data from Arnaud and Rothenflug (1985). The resulting temperatures are $1.5 \times 10^6$ K for $C^{6+}/C^{5+} = 1.8$, $2.0 \times 10^6$ K for $O^{8+}/O^{7+} = 0.22$, and $3.7 \times 10^6$ K for $Ne^{10+}/Ne^{9+} = 0.23$. The higher are the species ionization potentials, the hotter are the locations on the Sun they originate from.

B07 analyzed the CXO spectra of comets using calculated emission cross sections of H- and He-like ions that are formed after the electron capture from atomic hydrogen. This is the simplest quantum system that may be calculated. On the other hand, the ionization potential of H is not very different from that of $H_2O$ (13.6 and 12.6 eV, respectively), and these potentials are main parameters in the classic approximation of the single electron capture. B07 took into account dissociation of $H_2O$ and then OH and applied the Haser model (Haser, 1957) for the density distribution of $H_2O$, OH, O, and H. All these species are similar in their model of charge

exchange. However, velocities of H formed by photolysis of $H_2O$ and OH are higher than those of $H_2O$, OH, and O by an order of magnitude, and the densities of H are therefore low and may be neglected, especially taking into account that the $H_2O$ photolysis length in comets is comparable with the CXO aperture radii in the observations of comets (Table 1).

B07 fitted the observed CXO spectra of comets using abundances of eight ions as free parameters. Their approach looks very reasonable, and their ion ratios as well as those from Christian et al. (2010) for Comet 8P/Tuttle are given in Table 4.

There are significant differences between our ion ratios and those of B07. Mean values for both sets of the data may be compared with those recommended by Schwadron and Cravens (2000) that are based on theory and mass spectrometer studies. Our data agree better for all ion ratios.

In our fits, the signal from $Ne^{8+}$ near 920 eV is greater than that from $Ne^{9+}$ near 1020 eV in the spectra of all comets where these signals are detectable. However, B07 did not detect the former but observed the latter. We succeeded in detecting $Ne^{9+}$ only in two comets, and the mean $Ne^{10+}/Ne^{9+} = 0.23 \pm 0.11$ from our study.

It is difficult to judge why our results agree better with Schwadron and Cravens (2000) than those of B07. Maybe, the laboratory studies of charge exchange with $H_2O$ (Greenwood et al., 2000, 2001) are preferable to the calculations of charge exchange with H. The background spectra from the S1 back-illuminated chip in B07 are not perfect as well. We do not know if the data of B07 were corrected for the variation of the S3 sensitivity (Fig. 1) and for the variable spectral resolution. The spectra begin at 300 eV in B07, while our spectra are extended to 150 eV, and this helps to get more accurate values for $C^{5+}$. Based on the results from von Steiger et al. (2000) and Schwadron and Cravens (2000), we neglected a possible contribution from $N^{7+}$, and this is another source of the differences between our ion ratios and those in B07.

Overall, X-ray spectroscopy of comets using the CXO observations may be used as a tool for diagnostics of the solar wind composition at various points in the heliosphere. The developed methods for analysis of the CXO low-resolution spectra of comets make it possible to perform the quantitative spectroscopy with identification of the emission lines and determination of abundances of the solar wind ions that excite those lines. The retrieved ion abundances and their variations involve some ions that are poorly covered by the existing mass-spectrometers and extend our knowledge of the solar wind and its properties.

## 6. Conclusions

X-rays from comets originate in charge exchange between heavy ions in the solar wind and cometary species. Spectra of nine comets observed by the Chandra X-ray Observatory (CXO) are corrected for the background and analyzed using the time-dependent instrument sensitivity and the energy-dependent spectral resolution. X-ray emissions are extracted from the spectra in the range of 150–1100 eV using the $\chi^2$-fitting.

Production of X-rays varies in the observed comets by a factor of 500 from $4.4 \times 10^{13}$ erg $s^{-1}$ in Comet 73P to $2.2 \times 10^{16}$ erg $s^{-1}$ in Comet Ikeya–Zhang. The measured solar wind flow is scaled to 1 AU and varies within a factor of 20, being the weakest in Comet 73P and the strongest in 9P/Tempel 1. The retrieved X-ray line intensities vary by factors of 200 and $5 \times 10^4$, being compared within a comet and between the comets, respectively.

The major lines are attributed to emissions of the H- and He-like ions, and laboratory data on the excitation cross sections for these emissions (Greenwood et al., 2000) are used to convert the observed emission into abundances of heavy ions in the solar wind. Continuity equations for charge exchange in comets are solved analytically and result in relationships between the X-ray emissions and the ion fluxes.

The flux of $O^{7+}$ scaled to 1 AU varies within a factor of 35 with a mean value of $1.6 \times 10^4$ $cm^{-2}$ $s^{-1}$. The retrieved ratios of $O^{8+}/O^{7+}$, $C^{6+}/C^{5+}$, $Ne^{10+}/Ne^{9+}$, $C^{6+}/O^{7+}$, $N^{6+}/O^{7+}$, and $Ne^{9+}/O^{7+}$ demonstrate significant variations, while their mean values for O, C, and N agree with those recommended by Schwadron and Cravens (2000) for the slow and fast solar wind. The retrieved mean $Ne^{9+}/O^{7+} = 0.03$ and $Ne^{10+}/Ne^{9+} = 0.23$, while data on $Ne^{9+}$ and $Ne^{10+}$ are lacking in Schwadron and Cravens (2000).

The results are compared with the ion ratios from B07 that were obtained from the same CXO spectra of comets, and some significant differences are briefly discussed. The CXO observations of comets covered a great variety of the observing conditions, comets, and variable solar wind flow and its ion composition. All these issues have been discussed and retrieved in this work. CXO X-ray spectroscopy of comets is a diagnostic tool to study the composition of the solar wind and its variations.

## Acknowledgments

This work is supported by Grant 11.G34.31.0074 of the Russian Government to Moscow Institute of Physics and Technology (PhysTech) and V.A. Krasnopolsky.

## References

Arnaud, M., Rothenflug, R., 1985. An updated evaluation of recombination and ionization rates. Astron. Astrophys. Suppl. Ser. 60, 425–457.
Beiersdorfer, P. et al., 2003. Laboratory simulations of charge exchange-produced X-ray emission from comets. Science 300, 1558–1559.
Bodewits, D. et al., 2007. Spectral analysis of the Chandra comet survey. Astron. Astrophys. 469, 1183–1197.
Christian, D.J. et al., 2010. Chandra observations of Comets 8P/Tuttle and 17P/Holmes during solar minimum. Astrophys. J. Suppl. Ser. 187, 447–459.
Cochran, A.L., Schleicher, D.G., 1993. Observational constraints on the lifetime of cometary $H_2O$. Icarus 105, 235–253.
Cravens, T.E., 1997. Comet Hyakutake X-ray source: Charge transfer of solar wind heavy ions. Geophys. Res. Lett. 25, 105–108.
Cravens, T.E., 2002. X-ray emission from comets. Science 296, 1042–1045.
Dennerl, K., 2010. Charge transfer reactions. Space Sci. Rev. 157, 57–91.
Dennerl, K., Englhauser, J., Trümper, J., 1997. X-ray emissions from comets detected in the Roentgen X-ray Satellite all-sky survey. Science 277, 1625–1630.
Dennerl, K., Aschenbach, B., Burwitz, V., Englhauser, J., Lisse, C.M., Rodriguez-Pascual, P.M., 2003. A major step in understanding the X-ray generation in comets: Recent progress obtained with XMM-Newton. Proc. SPIE 4851, 277–288.
Dennerl, K. et al., 2006. First observation of Mars with XMM-Newton. Astron. Astrophys. 451, 709–722.
Greenwood, J.B., Williams, I.D., Smith, S.J., Chutjian, A., 2000. Measurement of charge exchange and X-ray emission cross sections for solar wind–comet interactions. Astrophys. J. 533, L175–L178.
Greenwood, J.B., Williams, I.D., Smith, S.J., Chutjian, A., 2001. Experimental investigation of the processes determining X-ray emission intensities from charge-exchange collisions. Phys. Rev. A 63. Article No: 062707, 9 pages.
Haser, L., 1957. Distribution d'intensite dans le tete d'une comete. Bul. Class Sci. Acad. Roy. Belgique 43, 740–750.
Hoekstra, R., Ciric, D., de Heer, F.J., Morgenstern, R., 1989. State-selective electron capture in collisions of $C^{6+}$ and $O^{8+}$ on atomic and molecular hydrogen studied by photon-emission spectroscopy. Phys. Scr. T28, 81–90.
Kharchenko, V., Dalgarno, A., 2001. Variability of cometary X-ray emission induced by solar wind ions. Astrophys. J. 554, L99–L102.
Kharchenko, V., Rigazio, M., Dalgarno, A., Krasnopolsky, V.A., 2003. Charge abundances of the solar wind ions inferred from cometary X-ray spectra. Astrophys. J. 585, L73–L75.
Krasnopolsky, V.A., 1997. On the nature of soft X-ray radiation in comets. Icarus 128, 368–385.
Krasnopolsky, V.A., 1998. Excitation of X-rays in Comet Hyakutake (C/1996 B2). J. Geophys. Res. 103, 2069–2075.
Krasnopolsky, V.A., 2006. X-rays and solar wind composition in four comets observed with Chandra X-ray Observatory. J. Geophys. Res. 111, A122102.
Krasnopolsky, V.A., Mumma, M.J., 2001. Spectroscopy of Comet Hyakutake at 80–700 Å: First detection of solar wind charge transfer emissions. Astrophys. J. 549, 629–634.
Krasnopolsky, V.A. et al., 1997. Detection of soft X-rays and a sensitive search for noble gases in Comet Hale–Bopp (C/1995 O1). Science 277, 1488–1491.

Krasnopolsky, V.A., Mumma, M.J., Abbott, M.J., 2000. EUVE search for X-rays from comets Encke, Mueller (C/1993 A1), Borrelly, and postperihelion Hale–Bopp. Icarus 146, 152–160.
Krasnopolsky, V.A., Christian, D.J., Kharchenko, V., Dalgarno, A., Wolk, S.J., Lisse, C.M., Stern, S.A., 2002. X-ray emission from Comet McNaught-Hartley (C/1999 T1). Icarus 160, 437–447.
Krasnopolsky, V.A., Greenwood, J.B., Stancil, P.C., 2004. X-ray and extreme ultraviolet emissions from comets. Space Sci. Rev. 113, 271–373.
Lisse, C.M. et al., 1996. Discovery of X-ray and extreme ultraviolet emission from Comet C/Hyakutake 1996 B2. Science 274, 205–209.
Lisse, C.M. et al., 2013. Chandra ACIS-S imaging spectroscopy of anomalously faint X-ray emission from Comet 103P/Hartley 2 during the EPOXI encounter. Icarus 222, 752–765.
Mumma, M.J., Krasnopolsky, V.A., Abbott, M.J., 1997. Soft X-rays from four comets observed with EUVE. Astrophys. J. 491, L125–L128.
Owens, A. et al., 1998. Evidence for dust-related X-ray emission from Comet C/1995 O1 (Hale–Bopp). Astrophys. J. 493, L47–L51.
Proposers' Observatory Guide, 2014. http://cxc.cfa.harvard.edu/proposer/POG/html.
Schwadron, N.A., Cravens, T.E., 2000. Implications of solar wind composition for cometary X-rays. Astrophys. J. 544, 558–566.
Suraud, M.G., Hoekstra, R., de Heer, F.J., Bonnet, J.J., Morgenstern, R., 1991. State selective electron capture into *nl* subshells in slow collisions of $C^{5+}$ and $N^{6+}$ with He and $H_2$ studied by photon emission spectroscopy. J. Phys. B 24, 2543–2558.
Von Steiger, R. et al., 2000. Composition of quasi-stationary solar wind flows from Ulysses/solar wind ion composition spectrometer. J. Geophys. Res. 105, 27217–27238.